E-shaped cantilever-based MEMS piezoelectric energy harvester for low frequency applications

SALEM SAADON[a,b*], OTHMAN SIDEK[b]
[a] *School of Electrical and Electronic Engineering, Universiti Sains Malaysia (USM),14300 NibongTebal, Pulau Pinang, Malaysia*
[b] *Collaborative Microelectronic Design Excellence Center (CEDEC), Universiti Sains Malaysia(USM), Engineering Campus 14300 Nibong Tebal, Seberang Perai Selatan, Pulau Pinang, Malaysia*

The simplicity associated with piezoelectric micro-generators makes them very attractive for MEMS applications in which ambient vibrations are harvested and converted into electric energy. These micro-generators can be an alternative to the battery-based solutions in the future, especially for remote systems. In this paper, we propose a model and present the simulation of a MEMS-based energy harvester under ambient vibration excitation using the coventorware2010 approaches. This E-shaped cantilever-based MEMS energy harvester that operates under ambient excitation in frequencies of 28, 29, and 31 Hz within a base acceleration of 1g produces an output current of 20 μA, 0.42 V, and a power of 0.2 μw at 5kΩ load.

(Received January 29, 2013; accepted March 13, 2014)

Keywords: Piezoelectric materials, Energy conversion, Shaped cantilever, MEMS

1. Introduction

In the last few years, many researchers have focused on a various geometrical shapes of piezoelectric cantilevers for the purpose of power optimization of the piezoelectric energy harvesters. In other words meeting the requirements to maximize the harvested power within the variations of cantilever dimensions, weight and cost is the main challenge to maintain the power capability at ambient vibration frequencies.

Previously, the rectangular shaped cantilevers were widely used due to their ease of fabrication, while the main disadvantage of such shape of cantilever is that the average strain is very poor.

In the last decade, most researchers have focused on the piezoelectric materials and the operating modes of the harvester rather than the geometrical shapes of the cantilever [1-11].

Saadon and Sidek [12], were proposed a brief literature review on micro scale rectangular cantilevered piezoelectric harvesters, they showed that the power harvested is not enough to be applicable.

Baker et al. [13], examined the effects of piezoelectric cantilever geometry on the power density in order to find a geometrical shape alternative to the popular rectangular shape.

Mateu and Moll [14] presented an analytical comparison between rectangular and triangular piezoelectric cantilevers having a large clamped end with a small free end. They were proved mathematically that, a triangular piezoelectric cantilever having a base and height similar to the base and length of a rectangular piezoelectric cantilever can withstand a higher strain as well as maximum deflection for a given boundary conditions of the beam.

Roundy et al. [15] discussed that the strain is uniformly distributed throughout the trapezoidal cantilever structure than a rectangular cantilever, they stated that, a trapezoidal piezoelectric cantilever could generate more than twice the energy that could be generated by a rectangular piezoelectric cantilever, provided that both cantilevers contain the same volume of PZT.

In this study a new E-shaped unimorph cantilever was designed and simulated in order to provide an optimized power as well as effective strain, by using coventorware approaches.

2. Factors affecting the optimization of harvested power

To achieve optimal output power of the cantilevered harvester, the resonant frequency should be taken into consideration. The dimensions of the cantilever and the mass decide the desirable resonant frequency of the harvester. Any slight deviation from the resonant frequency will cause a large reduction in the output power of such harvester. Thus, this resonant frequency should be calculated carefully to match the excitation frequency of the harvester and meet the optimal conditions for its output harvested power, which is the main objective of this paper.

To determine the value of resonant frequency of any cantilevered piezoelectric energy harvester, important parameters should be defined from its structure as denoted in Fig. 1.

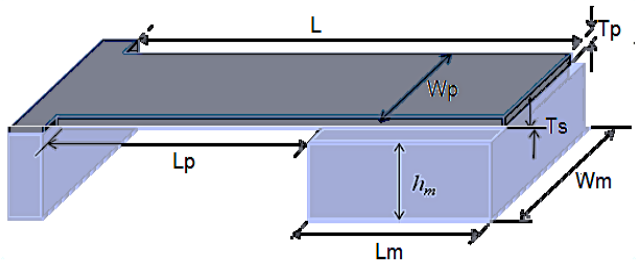

Fig. 1. Typical MEMS-based cantilevered piezoelectric energy harvester.

Usually, the resonant frequency of a piezoelectric cantilever is expressed by Equation (1) [16]

$$f_n = \frac{\upsilon_n^2}{2\pi l^2}\sqrt{\frac{EI}{m'}} \tag{1}$$

where f_n and ν_n are the nth mode of the resonant frequency and the eigenvalue respectively, l is the cantilever length, E is the modulus of elasticity (Young's modulus), I is the area moment of inertia about the neutral axis, and m' is the mass per unit length of the cantilever.

Equation1 can be rewritten in terms of the bending modulus per unit width (D_p) as follows:

$$f_n = \frac{\upsilon_n^2}{2\pi l^2}\sqrt{\frac{D_p}{m}} \tag{2}$$

$$m = \rho_p t_p + \rho_s t_s \tag{3}$$

A cantilever consists of two different material layers. Thus, the mass per unit area (m) is calculated by the sum of the products of the density and thickness of each layer. $\rho_p t_p$ is the product of the density and thickness of the piezoelectric layer, whereas $\rho_s t_s$ is the product of the density and thickness of the support layer.

As expressed by [17], the bending modulus D_p is a function of both Young's moduli and the thicknesses of the two layers, i.e.,

$$D_p = \frac{E_p^2 t_p^4 + E_s^2 t_s^4 + 2E_p E_s t_p t_s \left(2t_p^2 + 2t_s^2 + 3t_p t_s\right)}{12\left(E_p t_p + E_s t_s\right)} \tag{4}$$

Where E_p and E_s are the Young's moduli of the two materials, whereas t_p and t_s are the respective thicknesses.

The purpose of attaching a proof mass at the tip of the cantilever is to lower its resonant frequency and to provide a large displacement at the cantilever tip.

The resonant frequency in this case is calculated by Equation (5) [16]

$$f_r = \frac{\omega}{2\pi} = \frac{1}{2\pi}\sqrt{\frac{K}{m_e}} \tag{5}$$

Where ω, K, and m_e are the angular frequency, the spring constant at the tip, and the effective mass of the cantilever, respectively.

The resonant frequency approximation when the size of the attached proof mass is smaller than the cantilever length is expressed in [17] as:

$$f_n' = \frac{\upsilon_n'^2}{2\pi}\sqrt{\frac{K}{m_e + \Delta m}} \tag{6}$$

Where $\upsilon_n^2 = \upsilon_n'^2\sqrt{3/0.236}$, whereas the effective mass m_e = 0.236mwl, by considering the axial velocity that acts on the length or the width (w<<l). The spring constant K can be written as,

$$K = \frac{3D_p w_p}{l^3} \tag{7}$$

When the center of the proof mass has a concentrated load, its distance is $l_m/2$ from the tip, and the effective spring constant at this point is expressed by Equation (8) [18]

$$K' = K\left(\frac{l}{l - l_m/2}\right)^3 \tag{8}$$

Therefore, by substituting the spring constant (K) in Equation (7) with the effective spring constant (K'), the resonant frequency of the cantilever with a proof mass is expressed by Equation (9)

$$f_n = \frac{\upsilon_n^2}{2\pi}\sqrt{\frac{0.236 w_p D_p \left(l - l_m/2\right)^3}{0.236 m w_p l^7 + \Delta m l^3 \left(l - l_m/2\right)^3}}$$
$$\Delta m = \rho_m l_m w_m h_m \tag{9}$$

Thus, the low resonant frequency of the cantilever beam can be determined either by increasing the cantilever length or by attaching a larger proof mass at its tip.

Based on the aforementioned equations, the design of a cantilever-based piezoelectric harvester demands a beam with high mechanical strength against vibration, as well as a higher mass density to meet the high-efficiency requirement.

3. Modeling of E-shaped cantilever-based MEMS energy harvester

The finite element analysis was performed within coventorware 2010; this program allows the user to edit the materials database by inputting user-defined values for the material properties as shown in step (1) of the design flowchart shown in Fig. 2.

All the mentioned steps will be explained in details throughout the design and simulation steps on the coming sections.

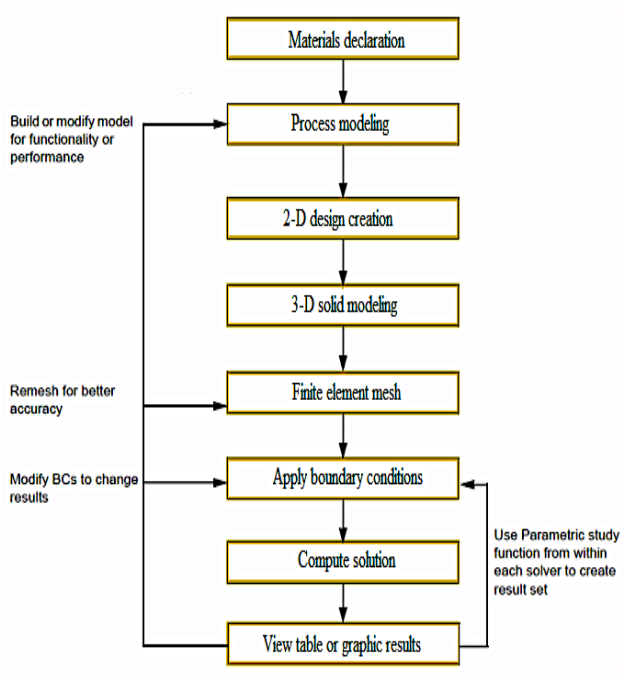

Fig. 2. Typical design flow.

3.1 Materials declaration

Some materials defined previously could be found in the materials database folder of the program, while some materials could be filled by the user, Two materials have been used in this design, such as Silicon and Lead zircon ate titan ate (PZT), whereas all the supported layer and the mass are of the same material (Si) due to the higher density of silicon, and a high electromechanical coupling of PZT compared to other piezoelectric materials.

Two main materials have been used throughout all processes, namely, PZT and silicon; their significant properties are presented in Table 1.

Table 1. Material properties of E-shaped piezoelectric cantilever.

Materials	Density (kg/μm^3)	Modulus of Elasticity (MPa)	Poisson's ratio
PZT	7.55e-15	8.9e+4	0.25
Silicon	2.5e-15	1.69e+5	0.3

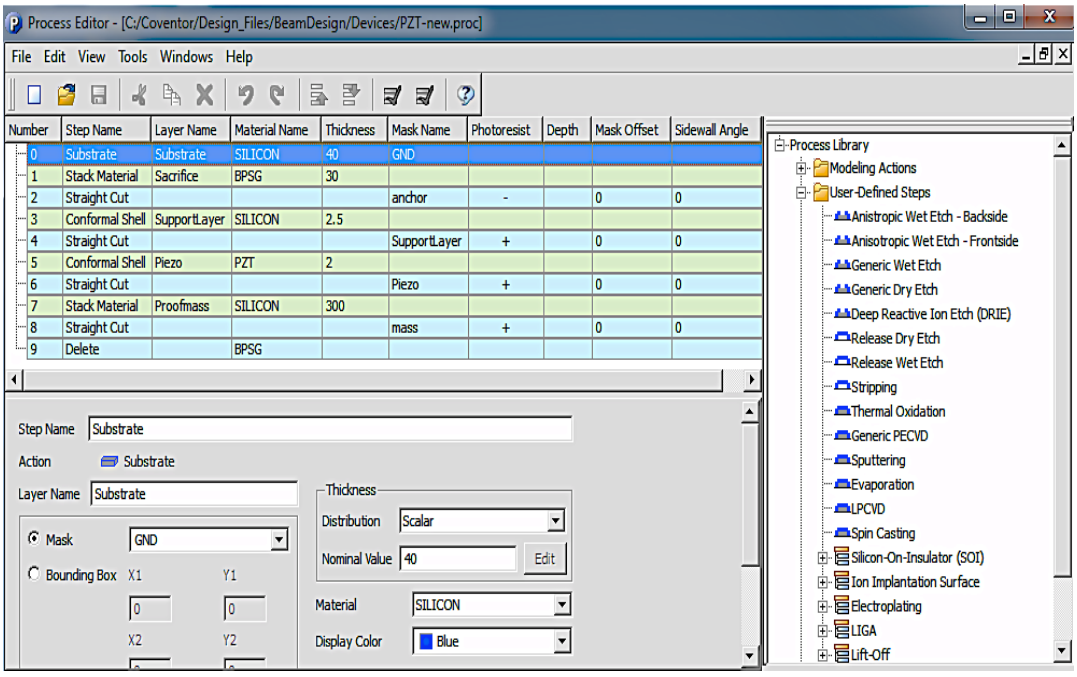

Fig. 3. Process editor of E-shaped cantilever.

3.2 Modeling processes

The masks are shown on the process editor window; all thicknesses of the layers were edited sequentially according to their location at the proposed design of the harvester from down to up.

The process name could be directly selected from the left side menu of the process editor as shown in Fig. 3.

3.3 Two-dimensional design creation

The X-Y dimensions layout of the E-shaped cantilevered harvester can be illustrated in Fig. 4; every mask layer has an individual color.

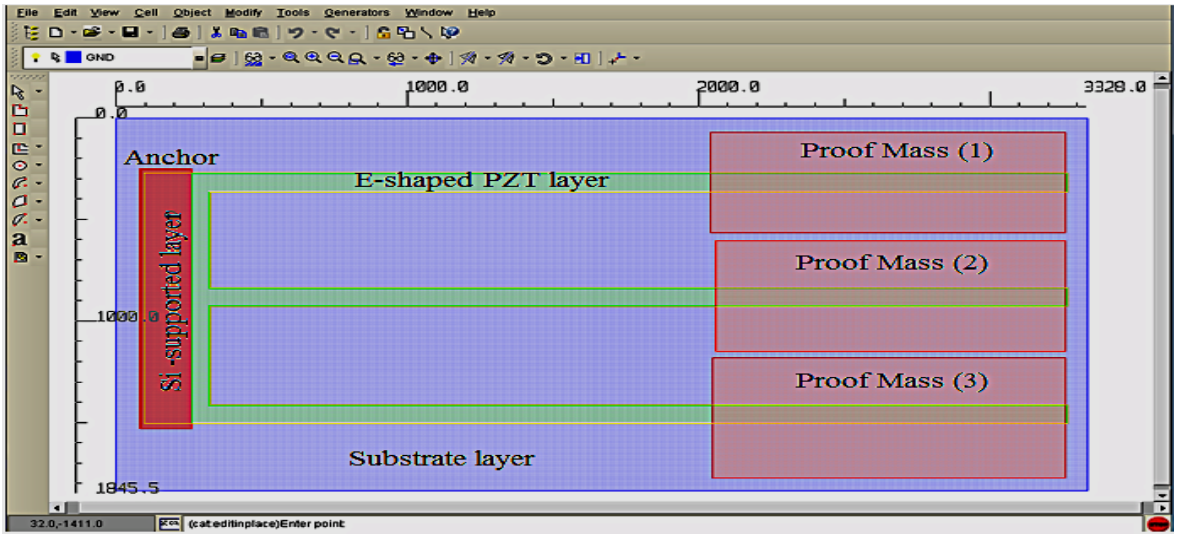

Fig. 4. X-Y dimensions of E-shaped cantilever.

The mask layers were arranged from down to top according to the process modeling shown in Fig. 4. The purpose of the anchor fixed at the substrate surface was to support all the cantilever layers of the system. The properties of each layer were defined previously at the process editor window, and their lengths and widths were read in microns from the implemented rulers at the X-Y dimensions.

This structure of the harvester is similar to the arrayed cantilever based structure of the previously discussed structures of several researchers, but in fact, here the proposed structure is more different, such that the coated piezoelectric layer PZT is deposited along all the supported layer structure, while in the case of arrayed cantilever it is deposited separately to each section of the array.

3.4 Three dimensions solid model and finite element meshing

The three dimensional design of the harvester in the processor window is illustrated in Fig. 5.

Since all thicknesses are in micron, the Z-scale was enlarged by 5 times for clarify.

For finite element meshing, the tetrahedral mesh type was used with parabolic element order and element size of 70 to all the specified layers.

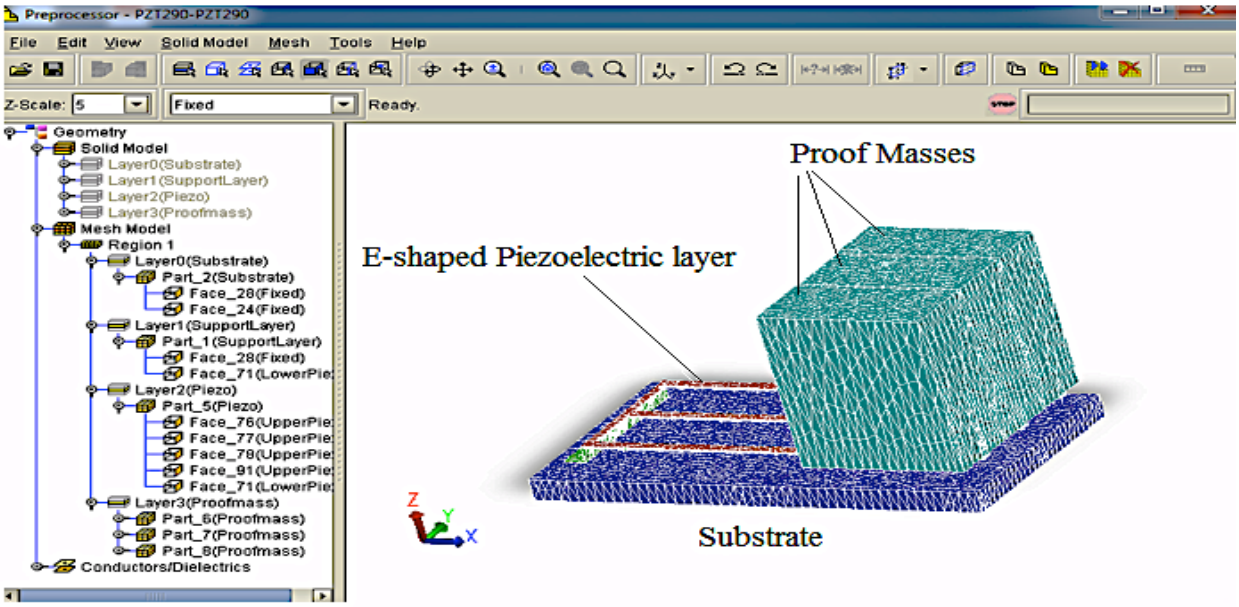

Fig. 5. Three dimensions of E-shaped cantilever.

3.5 Boundary conditions of the E-shaped harvester

The applied force and acceleration as boundary conditions that affect the deflection magnitude of the cantilever depend upon the proof mass size connected to the tip end and the base acceleration of the harvester.

The acceleration in this case adjusted to the normal gravitational acceleration of 9.81 m/s^2.

Three different values of load resistances were connected across the upper and lower surfaces of the piezoelectric material (PZT), that have values from 100 Ohms to several kilo Ohms to control the variation of the power harvested according to different loads.

4. Simulation results of E-shaped cantilever-based MEMS energy harvester

On the Analyzer/MemMech tab of the coventor2010; two types of simulations have been discussed through their obtained results as mentioned throughout the following sections.

4.1 Modal harmonic analysis results

There were three frequency modes (mode 1, mode 2 and mode 3) developed by this harvester as shown in Fig. 6.

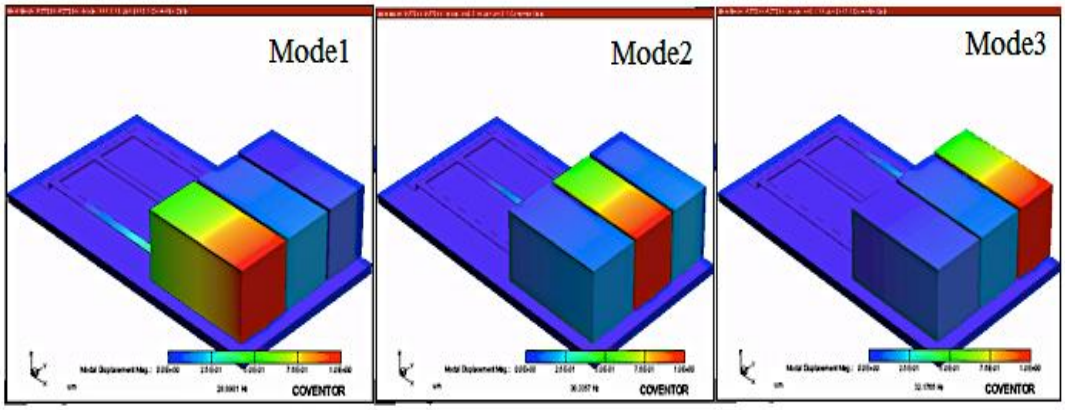

Fig. 6. Frequency modes of E-shaped cantilever.

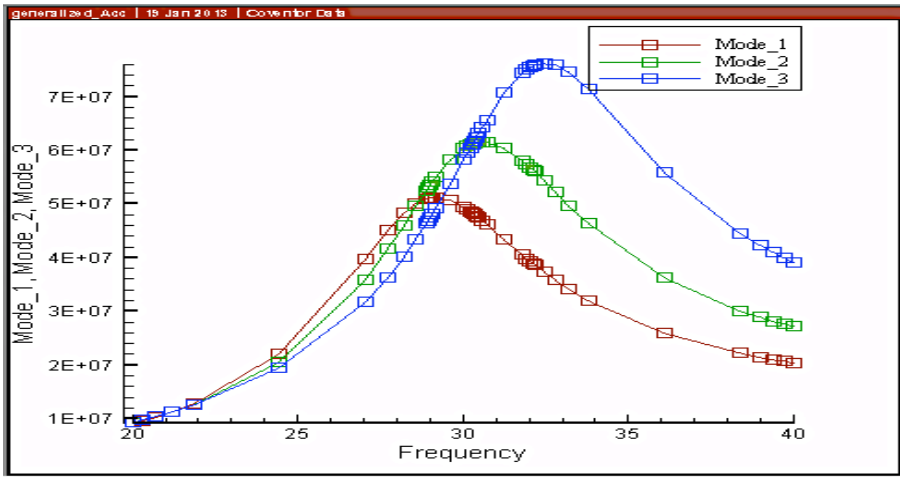

Fig. 7. Tip mass displacement vs. frequency of E-shaped cantilever.

The generalized displacement results obtained from these three modes with respect to the frequency variations are presented in Fig. 7.

The significant benefits of this E-shaped cantilever structure are a) the deflection effect of one cantilever part on the adjacent parts generates a wide frequency band, and b) enhanced harvested power due to the high strain developed.

4.2 Harmonic tip mass displacement results

The natural frequency is the frequency at which a maximum Z-displacement is occurred, as shown by the harmonic displacement window in Fig. 8 (a).

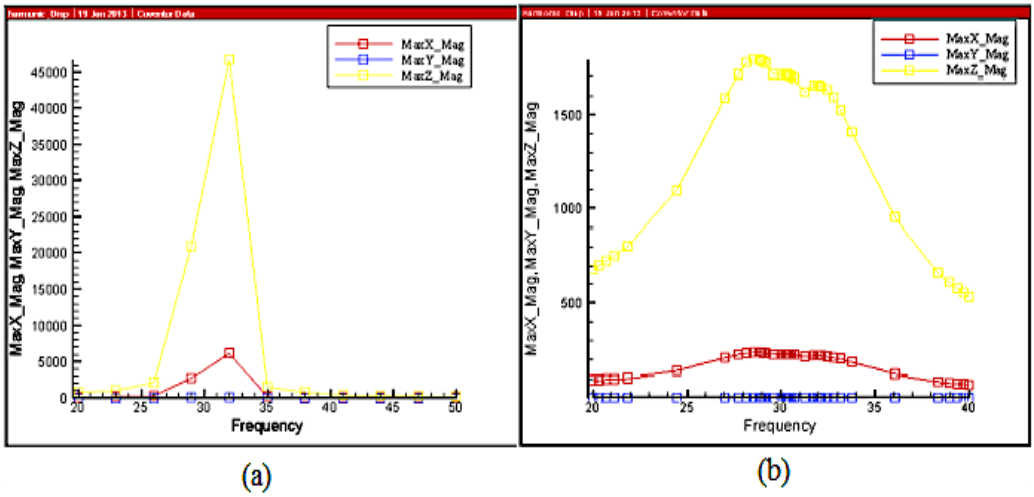

Fig. 8. Harmonic displacement versus frequency (a) harmonic displacement, and (b) generalized displacement.

The mode frequencies of the harvester due to the displacements in the three cantilever sections range from 25 to 35 Hz, those produce a displacement at Z-direction vary from 5000 to 45000 micron. The maximum displacement has occurred at a short circuit condition.

The harmonic generalized displacement magnitude is shown in Figure 8(b), which indicates three overall peak values of displacement at three resonant frequencies (28, 29 and 32 Hz) due to the displacement of the three cantilever branches.

4.3 Output voltage, current and power

Unlike tip displacement, output voltage is a function of the resistive load, as can be seen in Fig. 9 (a), in which the harmonic output voltage output response function for a various resistive loads includes the first three modes can be clearly illustrated. And the maximum generated voltage is about 0.42 volts, which is consistent with those obtained by previous researchers.

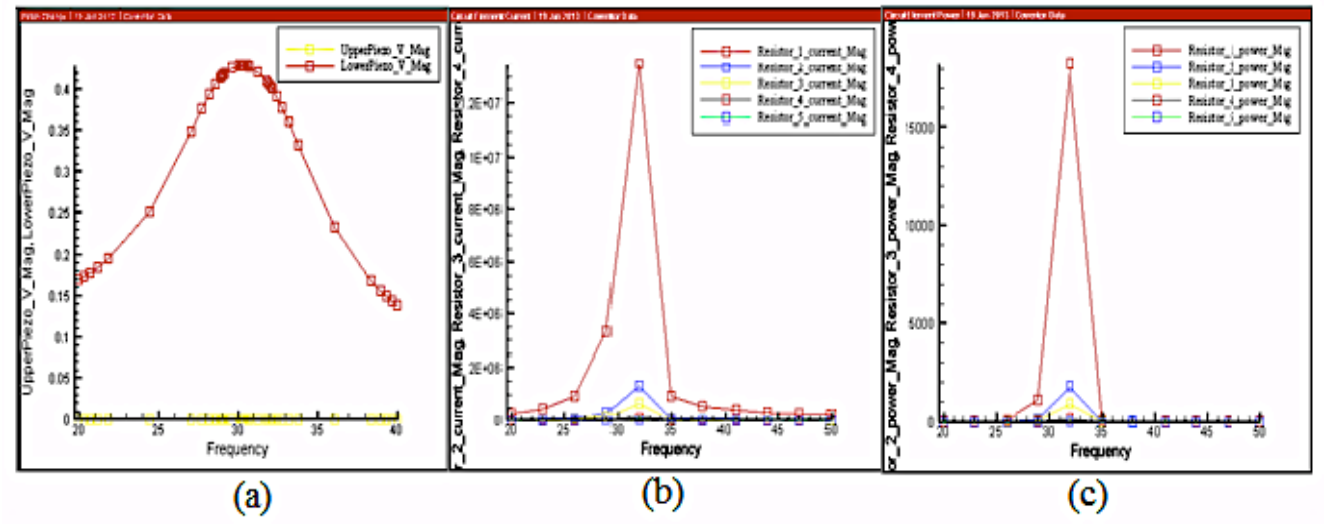

Fig. 9. Graphical output response: (a) output voltage, (b) output current, and (c) output power.

Usually, what designers care about is the power through the connected load (resistor).

These results show the current and the power frequency response functions of the proposed unimorph E-shaped cantilevered piezoelectric harvester, at given the various resistive loads, whose values vary between 100 ohms and 50 kilo-ohms as shown in Fig. 9 (b, c).

The Analyzer/MemMech results were generated for both current and power are in Pico Amperes and micro Watts units respectively.

From Fig. 9 (b, c), show that the plots of the current as well as the power response peaks for each resistive load are slightly different at the higher loads than the short circuit or at the loads in the range of several ohms.

5. Conclusion

The Analyzer/MemMech model predicted that the maximum obtained output voltage was in the open circuit limit, which was actually simulated using TiePotential

Surface BC. The predicted maximum voltage from the Analyzer/MemMech simulation is about 0.42 volts, which agrees with that obtained by previous researchers using MEMS scale simulations.

The power through the resistor is the most important in this study; since the maximum power was produced at the loads below the open circuit limit, the base acceleration amplitude would affect the power limitations of the harvester. The predicted power was 0.2 microwatts at the load of 5 kilo-ohms.

Thus, increasing the cantilever branches increases the frequency band of the harvester, but causes more difficulties in MEMS fabrication process.

Acknowledgements

This work is supported by Universiti Sains Malaysia (USM) fellowship and the Postgraduate Research Grant Scheme (PRGS), 1001/PELECT/8044039.

References

[1] M. Marzencki, S. Basrour, B. Charlot, A. Grasso, M. Colin, L. Valbin, DTIP'05, Montreux, Switzerland; June 01-03, 2005.
[2] M. Marzencki, Y. Ammar, S. Basrour, Sensors Actuat A – Phys. **145**, 363 (2008).
[3] D. Shen, J. H. Park, J. Ajitsaria, S. Y. Choe, H. C. Wikle, D. J. Kim, J Micromech Microeng; 18 (2008).
[4] M. Renaud, K. Karakaya, T. Sterken, P. Fiorini, C. Van Hoof, R. Puers, Sensors Actuat A – Phys. **145**, 380 (2008).
[5] H. B. Fang, J. Q. Liu, Z. Y. Xu, L. Dong, L. Wang, D. Chen, et al. Microelectron J **37**, 1280 (2006).
[6] J. Q. Liu, H. B. Fang, Z. Y. Xu, X. H. Mao, X. C. Shen, D. Chen, et al. Microelectron J **39**, 802 (2008).
[7] Y. B. Jeon, R. Sood, J. H. Jeong, S. G. Kim, Sensors Actuat A – Phys. **122**, 16 (2005).
[8] B. S. Lee, W. J. Wu, W. P. Shih, D. Vasic, F. Costa, In: 2007 IEEE ultrasonics symposium proceedings, **1-6**, 1598 (2007).
[9] B. S. Lee, S. C. Lin, W. J. Wu, X. Y. Wang, P. Z. Chang, C. K. Lee, J Micromech Microeng. 19 (2009).
[10] P. Muralt, M. Marzencki, B. Belgacem, F. Calame, S. Basrour, Procedia Chem. **1**, 1191 (2009).
[11] R. Elfrink, T. M. Kamel, M. Goedbloed, S. Matova, D. Hohlfeld, Y. van Andel, et al. J Micromech Microeng. 19 (2009).
[12] S. Saadon, O. Sidek, Energy Conversion and Management **52**, 500 (2011) .
[13] L. Mateu, F. Moll, J Intell Mater Syst Struct. **16**, 835 (2005).
[14] S. Roundy, E. S. Leland, J. Baker, E. Carleton, E. Reilly, E. Lai, et al. IEEE Pervasive Comput. **4**, 28 (2005).
[15] J. Baker, S. Roundy, P. Wright, In: Proceeding 3rd international energy conversion engineering conference, San Francisco, California; August 15-18, 2005.
[16] James M. Gere, Stephen P. Timoshenko, Mechanics of materials. 2nd. (1984), Belmont, Ca: Brooks/Cole Engineering.
[17] Yi, Jeong Woo, Shih, Wan Y. Shih, Wei-Heng, Journal of Applied Physics, **91**(3), 1680 (2002).
[18] J. E. Sader, I. Jarson, M. Paul, L. R. White, Rev. Sci. Instrum, **66**, 3789 (1995).

*Corresponding author: saadonsalem@yahoo.com